GEOLOGY | THE GEOLOGICAL SOCIETY OF AMERICA®

https://doi.org/10.1130/G47972.1

Manuscript received 2 June 2020
Revised manuscript received 9 July 2020
Manuscript accepted 14 August 2020

Published online 23 September 2020

A link between rift-related volcanism and end-Ediacaran extinction? Integrated chemostratigraphy, biostratigraphy, and U-Pb geochronology from Sonora, Mexico

Eben B. Hodgin[1]*, Lyle L. Nelson[2]*, Corey J. Wall[3], Arturo J. Barrón-Díaz[4], Lucy C. Webb[2], Mark D. Schmitz[3], David A. Fike[5], James W. Hagadorn[6] and Emily F. Smith[2]

[1]Department of Earth and Planetary Sciences, Harvard University, Cambridge, Massachusetts 02138, USA
[2]Department of Earth and Planetary Sciences, Johns Hopkins University, Baltimore, Maryland 21218, USA
[3]Department of Geosciences, Boise State University, Boise, Idaho 83725, USA
[4]Departamento de Geología, Universidad de Sonora (UNISON), Hermosillo 83000, Sonora, Mexico
[5]Department of Earth and Planetary Sciences, Washington University, St. Louis, Missouri 63130, USA
[6]Department of Earth Sciences, Denver Museum of Nature & Science, Denver, Colorado 80205, USA

ABSTRACT

We present chemostratigraphy, biostratigraphy, and geochronology from a succession that spans the Ediacaran-Cambrian boundary in Sonora, Mexico. A sandy hematite-rich dolostone bed, which occurs 20 m above carbonates that record the nadir of the basal Cambrian carbon isotope excursion within the La Ciénega Formation, yielded a maximum depositional age of 539.40 ± 0.23 Ma using U-Pb chemical abrasion–isotope dilution–thermal ionization mass spectrometry on a population of sharply faceted volcanic zircon crystals. This bed, interpreted to contain reworked tuffaceous material, is above the last occurrences of late Ediacaran body fossils and below the first occurrence of the Cambrian trace fossil *Treptichnus pedum*, and so the age calibrates key markers of the Ediacaran-Cambrian boundary. The temporal coincidence of rift-related flood basalt volcanism in southern Laurentia (>250,000 km^3 of basalt), a negative carbon isotope excursion, and biological turnover is consistent with a mechanistic link between the eruption of a large igneous province and end-Ediacaran extinction.

INTRODUCTION

The Ediacaran-Cambrian (E-C) boundary is one of the critical biological transitions in Earth history, marking the disappearance of Ediacaran organisms, a diverse assemblage of early macroscopic life forms, and the subsequent radiation of modern clades of metazoans. Continued efforts to understand the timing and extent of environmental and geochemical change across this boundary—and its potential role in driving extinction and evolution—are hampered by challenges in correlating and integrating records regionally and globally.

A large negative carbon isotope ($\delta^{13}C$) excursion, termed the basal Cambrian carbon isotope excursion (BACE), coincides with the E-C boundary in a number of regions globally (Magaritz et al., 1986; Narbonne et al., 1994; Brasier et al., 1996; Kimura et al., 1997; Zhang et al., 1997; Corsetti and Hagadorn, 2000; Amthor et al., 2003; Loyd et al., 2012). The BACE has been suggested as a formal marker of the E-C boundary (Zhu et al., 2019) and to be mechanistically linked to extinction (Kimura et al., 1997; Amthor et al., 2003). Currently, the best age constraint on this excursion is from the Ara Group of Oman, where an ash bed below the onset of a negative $\delta^{13}C$ excursion has been dated at 541.00 ± 0.13 Ma with U-Pb chemical abrasion–isotope dilution–thermal ionization mass spectrometry (CA-ID-TIMS) on zircon (Bowring et al., 2007). Correlation of these $\delta^{13}C$ excursions from localities around the world remains uncertain, and assessing the synchrony or duration of the BACE—necessary steps in considering its possible origins and consequences—requires improved radioisotopic age constraints.

*These authors contributed equally to this work. E-mails: ebenblake@berkeley.edu; lylelnelson@jhu.edu.

GEOLOGICAL BACKGROUND

The Caborca block in northwestern Mexico is composed of Mesoproterozoic basement (Anderson and Silver, 1981) and contains a well-exposed succession of Neoproterozoic–early Paleozoic shallow-marine strata (Fig. 1; Stewart et al., 1984) that record the E-C transition within the La Ciénega and Cerro Rajón Formations (Sour-Tovar et al., 2007; Loyd et al., 2012; Barrón-Díaz et al., 2019a). The La Ciénega Formation consists of four units. Unit 1 is composed of mixed dolostone, sandy dolostone, and siltstone to medium sandstone, and it contains 6 m of basalt at Cerro Rajón (Stewart et al., 1984). *Cloudina hartmannae* fossils occur within wackestone to packstone dolostone beds in the middle of Unit 1 (Stewart et al., 1984; Sour-Tovar et al., 2007). The uppermost part of Unit 1 is micaceous siltstone to fine sandstone with minor channels of medium quartz sandstone, and it is overlain by blue-weathering dolostone and minor sandy dolostone of Unit 2. Thin-bedded sandy dolostone and sandstone at the base of Unit 3 mark a conformable transition into micaceous siltstone to fine sandstone with minor beds of quartz sandstone, dolomite, sandy dolomite, and basalt. Unit 4 is massive buff-weathering dolostone with poorly developed stromatolites and oolite at the base. A previous report of *Cloudina* from Unit 4 (Sour-Tovar et al., 2007) has since been refuted (Loyd et al., 2012; Barrón-Díaz et al., 2019b). Loyd et al. (2012) identified a negative $\delta^{13}C$ anomaly in Units 2–4 with a nadir of –6.2‰ and correlated this with the BACE.

The La Ciénega Formation is overlain by the Cerro Rajón Formation, and the contact is a thin, locally preserved interval of siltstone to sandstone containing mud cracks and complex ichnofossils, including *Treptichnus pedum* (Loyd et al.,

CITATION: Hodgin, E.B., et al., 2021, A link between rift-related volcanism and end-Ediacaran extinction? Integrated chemostratigraphy, biostratigraphy, and U-Pb geochronology from Sonora, Mexico: Geology, v. 49, p. 115–119, https://doi.org/10.1130/G47972.1

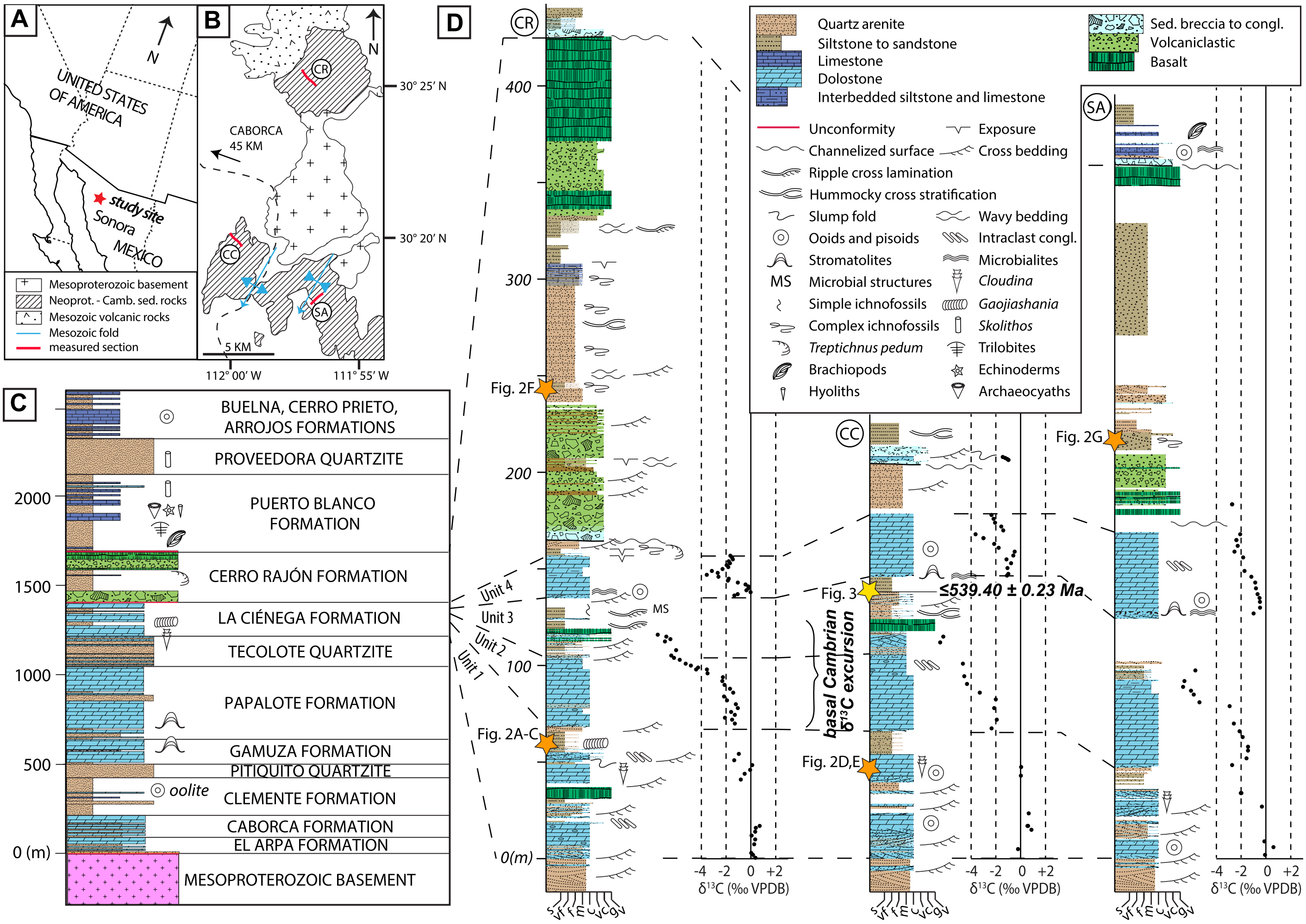

Figure 1. Locality map and integrated stratigraphy of the Ediacaran-Cambrian boundary near Caborca, northwestern Mexico. (A) Locality map with star marking the study site. (B) Geologic map showing distribution of Neoproterozoic–Cambrian strata and locations of measured sections; modified from Barrón-Díaz et al. (2019a). (C) Generalized Neoproterozoic–Cambrian lithostratigraphy and biostratigraphy, including data compiled from Stewart et al. (1984) and Barrón-Díaz et al. (2019a). (D) Integrated lithostratigraphy, biostratigraphy, δ^{13}C chemostratigraphy, and geochronology from measured sections, corresponding to Figure 1B. Neoprot.—Neoproterozoic; Camb.—Cambrian; CR—Cerro Rajón; CC—Cerro Clemente; SA—Cerro San Agustín; s—siltstone; vf—very fine-grained; f—fine-grained; m—medium-grained; c—coarse-grained; vc—very coarse-grained; g—conglomerate; v—volcanic; VPDB—Vienna Peedee belemnite; sed.—sedimentary; congl.—conglomerate.

2012; Barrón-Díaz et al., 2019a, 2019b). A boulder conglomerate disconformably overlies this sequence, erosively cutting down into Unit 4 of the La Ciénega Formation, and it contains dolostone, quartzite, and basalt clasts. The Cerro Rajón Formation contains variable proportions of siliciclastic, volcaniclastic, and volcanic rocks with minor silty to sandy limestone. The volcanic and volcaniclastic rocks are oceanic-island basalt–type enriched alkaline basalts characteristic of intraplate volcanism (Barrón-Díaz et al., 2019b). Abundant bed-parallel and more complex bed-penetrating ichnofossils occur within clastic facies throughout the Cerro Rajón Formation (Stewart et al., 1984; Sour-Tovar et al., 2007; Barrón-Díaz et al., 2019a), which is disconformably overlain by erosive conglomerate at the base of the Puerto Blanco Formation Unit 2 that, in turn, contains Cambrian Series 2 trilobites and brachiopods (Stewart et al., 1984; Sour-Tovar et al., 2007; Barrón-Díaz et al., 2019a).

METHODS

Field work conducted near Caborca, Mexico, included the measurement of stratigraphic sections of the La Ciénega and Cerro Rajón Formations at three localities (Figs. 1A and 1B). Carbonate samples were collected at 1–3 m intervals for carbon and oxygen stable isotope analyses. Zircon grains were separated from a sandy dolostone bed, imaged by cathodoluminescence (CL), and dated by laser ablation–inductively coupled plasma mass spectrometry (LA-ICPMS) and CA-ID-TIMS (see the Supplemental Material[1] for detailed methods).

[1]Supplemental Material. Section S1 (detailed methods), Section S2 (tuffaceous horizons in marine carbonates), Tables S1–S3, and Figures S1–S5. Please visit https://doi.org/10.1130/GEOL.S.12915629 to access the supplemental material, and contact editing@geosociety.org with any questions.

CHEMOSTRATIGRAPHY

Carbonate δ^{13}C values are ~0‰ in the lower dolostone of Unit 1 of the La Ciénega Formation, and decrease to below −6‰ within Unit 2 and to values as low as −7.5‰ in thin dolostone beds of Unit 3 interbedded with fine-grained siliciclastic rocks, before recovering to ~0‰ near the base of Unit 4 (Fig. 1D). Unit 4 contains a second negative excursion with values down to −3.6‰. These results were reproduced in three sections of the La Ciénega Formation (Fig. 1D; Table S1 in the Supplemental Material), and they closely resemble documented trends in coeval successions from Nevada (Corsetti and Hagadorn, 2003; Smith et al., 2016, 2017) and California (Corsetti and Hagadorn, 2000), demonstrating local to regional reproducibility of this δ^{13}C excursion.

Although the most negative δ^{13}C values at the nadir of the excursion correspond to a siliciclastic-rich interval, much of the excursion,

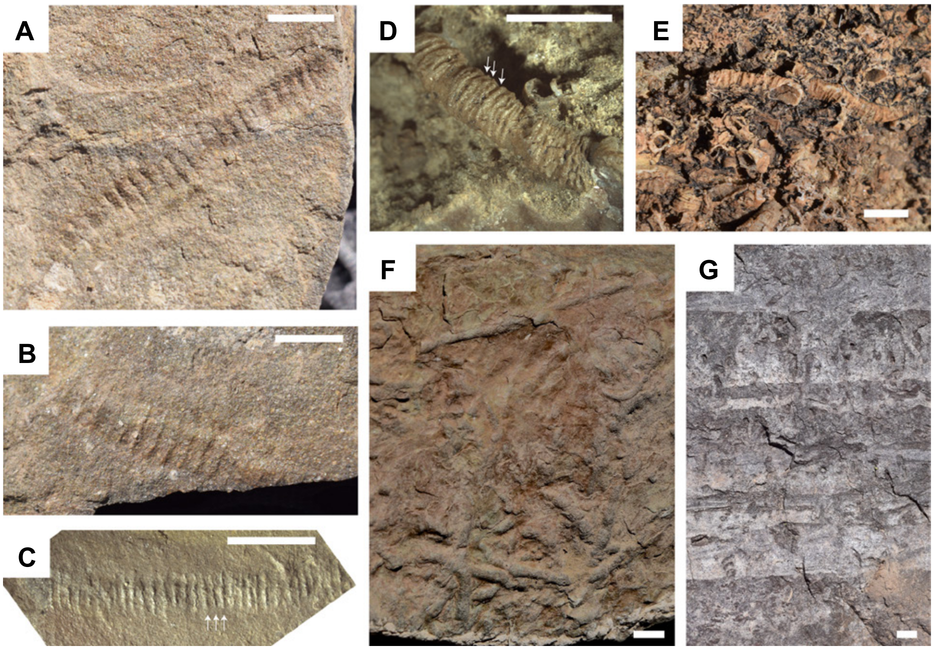

Figure 2. Photographs of fossils from La Ciénega and Cerro Rajón Formations, northwestern Mexico. Scale bars are 1 cm. Stratigraphic positions of specimens are shown in Figure 1D. (A) Cast of an annulated tubular body fossil in micaceous siltstone of the La Ciénega Formation, tentatively identified as *Gaojiashania* sp. (B) Mold of specimen in A. (C) Annulated tubular body fossil with rings lightly replaced by iron oxides in micaceous siltstone of the La Ciénega Formation, tentatively identified as *Gaojiashania* sp. Arrows highlight rings. (D) Silicified *Cloudina* in dolostone of the La Ciénega Formation; arrows highlight nested funnel structure. (E) Silicified *Cloudina* coquina in dolostone of the La Ciénega Formation (F) Complex bed-penetrating ichnofossils preserved on the bed sole within sandstone of the lower Cerro Rajón Formation. (G) Cross-section view of vertical to subvertical bed-penetrating ichnofossils within sandstone of the lower Cerro Rajón Formation.

including the decrease to ~–6‰, occurs within bedded dolo-grainstone. Isotopic values do not coherently vary with noticeable changes in lithology, depositional environment, or sequence boundaries, and δ^{13}C and δ^{18}O isotopes do not covary ($R^2 = 0.0025$; Fig. S1). Taken together, these characteristics suggest carbon isotopes were not reset by fluid-rock interactions related to meteoric diagenesis (Lohmann, 1988).

PALEONTOLOGY

Cloudina shell beds or coquina—preserved with varying degrees of silicification—occur at all three localities within dolostone beds of Unit 1 of the La Ciénega Formation and include examples of nested funnel structures (Figs. 2D and 2E; Sour-Tovar et al., 2007). Annulated tubular fossils preserved as casts and molds in siltstone of the upper part of Unit 1 of the La Ciénega Formation were tentatively identified as *Gaojiashania* based on the presence of densely spaced transverse rings, lack of tapering, and similarity in size and morphology to specimens documented in Nevada (Figs. 2A–2C; Smith et al., 2016, 2017). In one specimen, the rings are lightly replaced by iron oxides, likely pyrite pseudomorphs (Fig. 2C). Small, bed-planar ichnofossils occur in siliciclastic intervals of Unit 3 of the La Ciénega Formation, and more complex, bed-penetrating ichnofossils occur in siliciclastic horizons of the Cerro Rajón Formation (Figs. 2F and 2G; Stewart et al., 1984; Sour-Tovar et al., 2007; Barrón-Díaz et al., 2019a).

GEOCHRONOLOGY

U-Pb geochronological analyses were obtained from a 10-cm-thick bed of sandy hematite-rich dolostone near the top of Unit 3 of the La Ciénega Formation at Cerro Clemente (Fig. 1D; Fig. S2). The bed is well laminated with a matrix consisting of fine-grained peloidal dolomicrite containing subordinate hematite, secondary silica, and clay (Fig. S2). Secondary mineral infilling of original porosity and hematization of clay minerals may be related to similar features observed in diagenetically altered tuffaceous horizons in marine carbonates (e.g., Kiipli et al., 2000; see the Supplemental Material). Redeposited material within the bed includes rounded grains of holoclastic quartz and accidental lithics of basement-derived metamorphic rock fragments (Fig. S2).

Screening of zircons by LA-ICPMS (130 analyses) yielded age populations at 540, 1000–1100, 1400–1500, and 1700–1800 Ma (Fig. S3A; Table S2), each defining discordia lines toward a Pb loss event at ca. 60 Ma, corresponding to the timing of metasomatism and greenschist-facies metamorphism related to Laramide orogenesis (Figs. S3B–S3D; Barrón-Díaz et al., 2019c). The ca. 540 Ma crystals have characteristics of a rift-related volcanic source, including consistent temperature-correlated differentiation trends in trace-element geochemistry (Fig. S4), inclusions of apatite and glass, and subdued internal oscillatory and sector zoning in an overall intense CL response (Fig. 3; Fig. S5). Six sharply faceted zircon grains were selected for CA-ID-TIMS analysis (Fig. 3D), with four grains split in half, yielding 10 zircon analyses. Six fragments with reproducible ^{206}Pb/^{238}U dates yielded a weighted mean age of 539.40 ± 0.23/0.35/0.66 Ma (2σ internal/2σ internal and tracer/2σ internal, tracer, and decay constant uncertainties; Figs. 3A–3C; Table S3; mean square weighted deviation = 1.05; probability of fit = 0.34), which we report conservatively as a maximum depositional age, but with a high probability of deposition close to eruption.

DISCUSSION AND CONCLUSIONS

The 539.40 ± 0.23 Ma dated horizon occurs ~20 m above the nadir and below the recovery from a negative δ^{13}C excursion that is reproduced across all three sections of the La Ciénega Formation (Fig. 1D), providing a maximum age constraint on the nadir of the BACE. Minimal evidence for facies dependence of δ^{13}C values or alteration by meteoric diagenesis and the reproducibility of the BACE along the southwestern Laurentian margin through variable lithologies and across stratigraphic sequence boundaries (Corsetti and Hagadorn, 2000, 2003; Smith et al., 2016, 2017) suggest a marine carbon cycle perturbation at the E-C boundary, rather than a diagenetic origin. By contrast, at Farm Swartpunt in Namibia, there is an ~140 m section of strata with dated ash beds (Linnemann et al., 2019) that overlap with the 539.40 ± 0.23 Ma age of the dated horizon in Sonora, and yet, there, the δ^{13}C values of carbonates remain stable at ~1‰ (Saylor et al., 1998). If the date reported here is a near-depositional age, as we suggest, then the BACE was not recorded on some margins, which could be explained by the existence of local, isotopically distinct pools of dissolved inorganic carbon (Swart et al., 2009; Geyman and Maloof, 2019). While the 541.00 ± 0.13 Ma age below the δ^{13}C excursion in Oman is ~1.5 m.y. older (Bowring et al., 2007), this may not directly date the onset of the BACE because the Ara Group was deposited in an evaporitic basin with probable depositional hiatuses (e.g., Zhu et al., 2019). Additional geochronology from strata containing this excursion will thus be necessary to test its global synchrony, duration, and synoptic variability, and to evaluate possible regional controls (Fig. 4).

In addition to calibrating the chemostratigraphic record in Sonora, the dated horizon

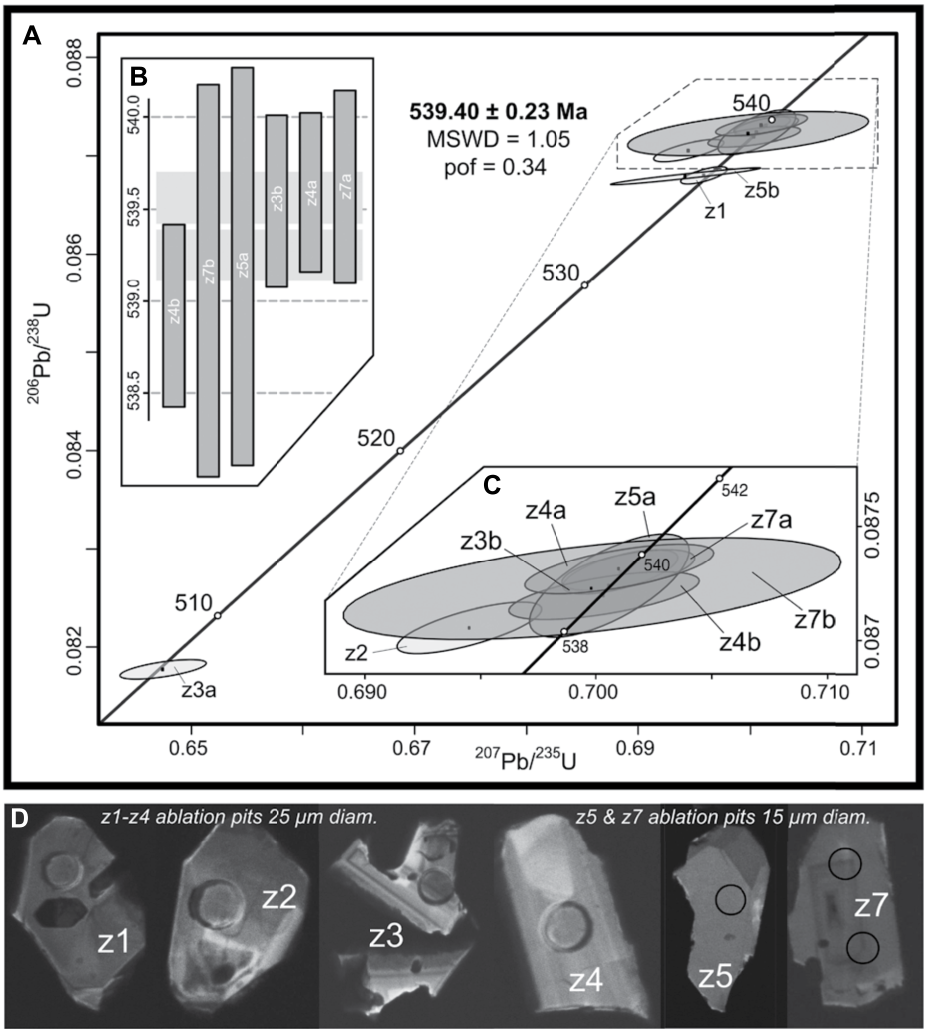

Figure 3. U-Pb zircon geochronology from sample CC1801–138 reported with 2σ internal uncertainty. Stratigraphic position is shown in Figure 1D. (A) Chemical abrasion–isotope dilution–thermal ionization mass spectrometry (CA-ID-TIMS) U-Pb concordia plot. (B) Age-rank plot of zircon fractions used to calculate weighted mean. (C) Concordia inset of zircon fractions used to calculate weighted mean. (D) Cathodoluminescence images of zircons analyzed by CA-ID-TIMS. MSWD—mean square weighted deviation; pof—probability of fit.

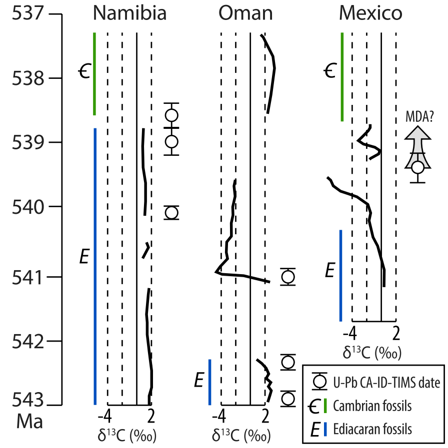

Figure 4. Compiled age constraints on the Ediacaran-Cambrian boundary from Namibia (Saylor et al., 1998; Linnemann et al., 2019), Oman (Amthor et al., 2003; Bowring et al., 2007), and Mexico. MDA—maximum depositional age; CA-ID-TIMS—chemical abrasion–isotope dilution–thermal ionization mass spectrometry.

occurs above the last stratigraphic occurrences of the Ediacaran fossils *Cloudina* and *Gaojiashania* and below the first occurrence of *Treptichnus pedum* in this region. This new date from Sonora is within error of the age range (538.99 ± 0.21 Ma to 538.58 ± 0.19 Ma) recently proposed for the E-C boundary at Swartpunt, Namibia, based on the last occurrences of Ediacaran body fossils and the first occurrences of *Treptichnus pedum* and other complex trace fossils (Fig. 4; Linnemann et al., 2019). Although biostratigraphic overlap between cloudinids and clades classically interpreted as Cambrian has been documented in Siberia and Mongolia (Zhu et al., 2017; Yang et al., 2020), confirmation of biostratigraphic correlation between Namibia and Mexico with U-Pb geochronology is consistent with hypotheses of globally synchronous biotic turnover and extinction of Ediacaran clades at the E-C boundary.

The dated horizon in Sonora occurs among basaltic rocks with an enriched mantle source that have been linked to rift-related volcanism within the Caborca block (Stewart et al., 1984; Barrón-Díaz et al., 2019b). Trace element geochemistry from the ca. 540 Ma zircon population is consistent with a mantle-derived source (Fig. S4; Grimes et al., 2015). The 539.40 ± 0.23 Ma age of this zircon population coincides with bimodal rift-related volcanism in southwestern Oklahoma (USA) that evolved from a magma source of similar composition and mineralogy (Barrón-Díaz et al., 2019b), and spanned from 539 to 530 Ma (Thomas et al., 2012), with an initial magmatic pulse resolved by CA-ID-TIMS at ca. 539.5 to 539.0 Ma (Wall et al., 2020). The volume of these early Cambrian basaltic lavas has been estimated at >250,000 km^3 and interpreted as a flood basalt province associated with rifting of the southern margin of Laurentia (Hanson et al., 2013; Brueseke et al., 2016).

In southwestern North America, the last appearance of Ediacaran fossils consistently occurs beneath the nadir of the BACE (Smith et al., 2016, 2017). Here, new geochronology demonstrates temporal coincidence of this biotic turnover, the BACE, and a pulse of volumetrically significant rift-related flood basalt volcanism. We suggest that there is a mechanistic link between this magmatism and environmentally driven extinction at the E-C boundary through alteration of marine chemistry and/or climate and a perturbation to the carbon cycle through isotopically light carbon inputs from volcanic outgassing and combusted organic carbon—perhaps analogous to links between the Central Atlantic Magmatic Province and the Triassic-Jurassic mass extinction during the breakup of Pangea (Schoene et al., 2010; Ruhl et al., 2011).

ACKNOWLEDGMENTS

We are grateful to A. Lizarraga for property access; J. Ramezani and I. Bennett (Massachusetts Institute of Technology, USA) and R. Mundil (Berkeley Geochronology Center, California, USA) for mineral separation assistance; J. Crowley (Boise State University, Idaho, USA) and G. Seward, F. Apen, A. Kylander-Clark, and F. Macdonald (University of California–Santa Barbara, USA) for U-Pb geochronology assistance; D. Brenner (Johns Hopkins University [JHU], Maryland, USA) and S. Moore (Washington University, St. Louis, Missouri, USA) for stable isotope analysis assistance; and Beck for field assistance. Our funding sources included U.S. National Science Foundation (NSF) Graduate Research Fellowship Program grant DGE-1746891 and National Geographic Early Career grant CP-002ER-17 to L.L. Nelson; NSF EAR-1827669 and support from the JHU Department of Earth and Planetary Sciences to E.F. Smith; and support from Harvard University to E.B. Hodgin. Constructive reviews from F. Bowyer, M. Zhu, and A. Prave improved this manuscript.

REFERENCES CITED

Amthor, J.E., Grotzinger, J.P., Schröder, S., Bowring, S.A., Ramezani, J., Martin, M.W., and Matter, A., 2003, Extinction of *Cloudina* and *Namacalathus* at the Precambrian-Cambrian boundary in Oman: Geology, v. 31, p. 431–434, https://doi.org/10.1130/0091-7613(2003)031<0431:EOCANA>2.0.CO;2.

Anderson, T., and Silver, L., 1981, An overview of Precambrian rocks in Sonora: Revista Mexicana de Ciencias Geológicas, v. 5, p. 131–139.

Barrón-Díaz, A.J., Paz-Moreno, F.A., and Hagadorn, J.W., 2019a, The Cerro Rajón Formation—A new lithostratigraphic unit proposed for a Cambrian (Terreneuvian) volcano-sedimentary succession from the Caborca region, northwest Mexico: Journal of South American Earth Sciences, v. 89, p. 197–210, https://doi.org/10.1016/j.jsames.2018.11.003.

Barrón-Díaz, A.J., Paz-Moreno, F.A., Lozano-Santa Cruz, R., Herrera-Urbina, S., Centeno-García, E., and López-Martínez, M., 2019b, Early Cambrian alkaline volcanism on the southern margin of Laurentia: Evidence in the volcaniclastic units from the Puerto Blanco Formation in the Caborca block, NW Mexico: International Geology Review, v. 61, p. 1189–1206, https://doi.org/10.1080/00206814.2018.1501619.

Barrón-Díaz, A.J., Paz Moreno, F.A., Miggins, D.P., and Iriondo, A., 2019c, Geochronology and geothermometry of the Laramide metamorphism in the Cambrian metabasalts from the Cerro Rajón Formation, Caborca region, northwest Mexico: Journal of South American Earth Sciences, v. 91, p. 47–56, https://doi.org/10.1016/j.jsames.2019.01.005.

Bowring, S.A., Grotzinger, J.P., Condon, D.J., Ramezani, J., Newall, M.J., and Allen, P.A., 2007, Geochronologic constraints on the chronostratigraphic framework of the Neoproterozoic Huqf Supergroup, Sultanate of Oman: American Journal of Science, v. 307, p. 1097–1145, https://doi.org/10.2475/10.2007.01.

Brasier, M.D., Shields, G., Kuleshov, V.N., and Zhegallo, E.A., 1996, Integrated chemo- and biostratigraphic calibration of early animal evolution: Neoproterozoic–early Cambrian of southwest Mongolia: Geological Magazine, v. 133, p. 445–485, https://doi.org/10.1017/S0016756800007603.

Brueseke, M.E., Hobbs, J.M., Bulen, C.L., Mertzman, S.A., Puckett, R.E., Walker, J.D., and Feldman, J., 2016, Cambrian intermediate-mafic magmatism along the Laurentian margin: Evidence for flood basalt volcanism from well cuttings in the Southern Oklahoma aulacogen (U.S.A.): Lithos, v. 260, p. 164–177, https://doi.org/10.1016/j.lithos.2016.05.016.

Corsetti, F.A., and Hagadorn, J.W., 2000, Precambrian-Cambrian transition: Death Valley, United States: Geology, v. 28, p. 299–302, https://doi.org/10.1130/0091-7613(2000)28<299:PTDVUS>2.0.CO;2.

Corsetti, F.A., and Hagadorn, J.W., 2003, The Precambrian-Cambrian transition in the southern Great Basin: The Sedimentary Record, v. 1, p. 4–8, https://doi.org/10.2110/sedred.2003.1.4.

Geyman, E.C., and Maloof, A.C., 2019, A diurnal carbon engine explains ^{13}C-enriched carbonates without increasing the global production of oxygen: Proceedings of the National Academy of Sciences of the United States of America, v. 116, p. 24433–24439, https://doi.org/10.1073/pnas.1908783116.

Grimes, C.B., Wooden, J.L., Cheadle, M.J., and John, B.E., 2015, "Fingerprinting" tectono-magmatic provenance using trace elements in igneous zircon: Contributions to Mineralogy and Petrology, v. 170, p. 1–26, https://doi.org/10.1007/s00410-015-1199-3.

Hanson, R.E., Puckett, R.E., Keller, G.R., Brueseke, M.E., Bulen, C.L., Mertzman, S.A., Finegan, S.A., and McCleery, D.A., 2013, Intraplate magmatism related to opening of the southern Iapetus Ocean: Cambrian Wichita igneous province in the Southern Oklahoma rift zone: Lithos, v. 174, p. 57–70, https://doi.org/10.1016/j.lithos.2012.06.003.

Kiipli, E., Kallaste, T., and Kiipli, T., 2000, Hematite and goethite in Telychian marine red beds of the East Baltic: GFF, v. 122, p. 281–286, https://doi.org/10.1080/11035890001223281.

Kimura, H., Matsumoto, R., Kakuwa, Y., Hamdi, B., and Zibaseresht, H., 1997, The Vendian-Cambrian $\delta^{13}C$ record, north Iran: Evidence for overturning of the ocean before the Cambrian explosion: Earth and Planetary Science Letters, v. 147, p. E1–E7, https://doi.org/10.1016/S0012-821X(97)00014-9.

Linnemann, U., Ovtcharova, M., Schaltegger, U., Gärtner, A., Hautmann, M., Geyer, G., Vickers-Rich, P., Rich, T., Plessen, B., Hofmann, M., and Zieger, J., 2019, New high-resolution age data from the Ediacaran-Cambrian boundary indicate rapid, ecologically driven onset of the Cambrian explosion: Terra Nova, v. 31, p. 49–58, https://doi.org/10.1111/ter.12368.

Lohmann, K.C., 1988, Geochemical patterns of meteoric diagenetic systems and their application to studies of paleokarst, *in* James, N.P., and Choquette, P.W., eds., Paleokarst: New York, Springer, p. 58–80, https://doi.org/10.1007/978-1-4612-3748-8_3.

Loyd, S.J., Marenco, P.J., Hagadorn, J.W., Lyons, T.W., Kaufman, A.J., Sour-Tovar, F., and Corsetti, F.A., 2012, Sustained low marine sulfate concentrations from the Neoproterozoic to the Cambrian: Insights from carbonates of northwestern Mexico and eastern California: Earth and Planetary Science Letters, v. 339, p. 79–94, https://doi.org/10.1016/j.epsl.2012.05.032.

Magaritz, M., Holser, W.T., and Kirschvink, J.L., 1986, Carbon-isotope events across the Precambrian/Cambrian boundary on the Siberian Platform: Nature, v. 320, p. 258–259, https://doi.org/10.1038/320258a0.

Narbonne, G.M., Kaufman, A.J., and Knoll, A.H., 1994, Integrated chemostratigraphy and biostratigraphy of the Windermere Supergroup, northwestern Canada: Implications for Neoproterozoic correlations and the early evolution of animals: Geological Society of America Bulletin, v. 106, p. 1281–1292, https://doi.org/10.1130/0016-7606(1994)106<1281:ICABOT>2.3.CO;2.

Ruhl, M., Bonis, N.R., Reichart, G.J., Sinninghe Damsté, J.S., and Kürschner, W.M., 2011, Atmospheric carbon injection linked to end-Triassic mass extinction: Science, v. 333, p. 430–434, https://doi.org/10.1126/science.1204255.

Saylor, B.Z., Kaufman, A.J., Grotzinger, J.P., and Urban, F., 1998, A composite reference section for terminal Proterozoic strata of southern Namibia: Journal of Sedimentary Research, v. 68, p. 1223–1235, https://doi.org/10.2110/jsr.68.1223.

Schoene, B., Guex, J., Bartolini, A., Schaltegger, U., and Blackburn, T.J., 2010, Correlating the end-Triassic mass extinction and flood basalt volcanism at the 100 ka level: Geology, v. 38, p. 387–390, https://doi.org/10.1130/G30683.1.

Smith, E.F., Nelson, L.L., Strange, M.A., Eyster, A.E., Rowland, S.M., Schrag, D.P., and Macdonald, F.A., 2016, The end of the Ediacaran: Two new exceptionally preserved body fossil assemblages from Mount Dunfee, Nevada, USA: Geology, v. 44, p. 911–914, https://doi.org/10.1130/G38157.1.

Smith, E.F., Nelson, L.L., Tweedt, S.M., Zeng, H., and Workman, J.B., 2017, A cosmopolitan late Ediacaran biotic assemblage: New fossils from Nevada and Namibia support a global biostratigraphic link: Proceedings of the Royal Society: B, Biological Sciences, v. 284, p. 1–10, https://doi.org/10.1098/rspb.2017.0934.

Sour-Tovar, F., Hagadorn, J.W., and Huitrón-Rubio, T., 2007, Ediacaran and Cambrian index fossils from Sonora, Mexico: Palaeontology, v. 50, p. 169–175, https://doi.org/10.1111/j.1475-4983.2006.00619.x.

Stewart, J.H., McMenamin, M.A.S., and Morales-Ramirez, J.M., 1984, Upper Proterozoic and Cambrian Rocks in the Caborca Region, Sonora, Mexico—Physical Stratigraphy, Biostratigraphy, Paleocurrent Studies and Regional Relations: U.S. Geological Survey Professional Paper 1309, 36 p., https://doi.org/10.3133/pp1309.

Swart, P.K., Reijmer, J.J.G., and Otto, R., 2009, A reevaluation of facies on Great Bahama Bank II: Variations in the $\delta^{13}C$, $\delta^{18}O$ and mineralogy of surface sediments, *in* Swart, P.K., et al., eds., Perspectives in Carbonate Geology: International Association of Sedimentologists Special Publication 41, p. 47–59.

Thomas, W.A., Tucker, R.D., Astini, R.A., and Denison, R.E., 2012, Ages of pre-rift basement and synrift rocks along the conjugate rift and transform margins of the Argentine Precordillera and Laurentia: Geosphere, v. 8, p. 1366–1383, https://doi.org/10.1130/GES00800.1.

Wall, C.J., Hanson, R.E., Schmitz, M., Price, J.D., Donovan, R.N., Boro, J.R., Eschberger, A.M., and Toews, C.E., 2020, Integrating zircon trace element geochemistry and high precision U-Pb zircon geochronology to resolve timing and petrogenesis of the late Ediacaran–Cambrian Wichita Igneous Province, Southern Oklahoma Aulacogen, USA: Geology, v. 48, https://doi.org/10.1130/G48140.1 (in press).

Yang, B., Steiner, M., Schiffbauer, J.D., Selly, T., Wu, X., Zhang, C., and Liu, P., 2020, Ultrastructure of Ediacaran cloudinids suggests diverse taphonomic histories and affinities with non-biomineralized annelids: Scientific Reports, v. 10, p. 1–10, https://doi.org/10.1038/s41598-019-56317-x.

Zhang, J., Li, G., Zhou, C., Zhu, M., and Yu, Z., 1997, Carbon isotope profiles and their correlation across the Neoproterozoic-Cambrian boundary interval on the Yangtze Platform, China: Bulletin of the National Museum of Natural Science, v. 10, p. 107–116.

Zhu, M., Zhuravlev, A.Y., Wood, R.A., Zhao, F., and Sukhov, S.S., 2017, A deep root for the Cambrian explosion: Implications of new bio- and chemostratigraphy from the Siberian Platform: Geology, v. 45, p. 459–462, https://doi.org/10.1130/G38865.1.

Zhu, M., Yang, A., Yuan, J., Li, G., Zhang, J., Zhao, F., Ahn, S.Y., and Miao, L., 2019, Cambrian integrative stratigraphy and timescale of China: Science China–Earth Sciences, v. 62, p. 25–60, https://doi.org/10.1007/s11430-017-9291-0.

Printed in USA